

Optical kinks and kink-kink and kink-pulse interactions in resonant two-level media

Denis V. Novitsky*

*B. I. Stepanov Institute of Physics, National Academy of Sciences of Belarus,
Nezavisimosti Avenue 68, BY-220072 Minsk, Belarus*

(Dated: September 30, 2021)

An optical kink is a shock-wave-like field structure which can appear in a resonant two-level medium as a result of the nonlinear process of self-steepening. We numerically simulate this process using an adiabatically switching waveform as an input and confirm the self-similarity of resulting kinks. The analysis is also applicable to a more general waveform with a decaying trailing edge which we call a kinklike pulse. We study in detail collisions of kinks with other kinks and ultrashort pulses and demonstrate the possibility to control kink speed by changing the parameters of counter-propagating fields. The effects considered can be treated as belonging to a wide class of unexplored phenomena in the regime of incoherent light-matter interaction.

PACS numbers: 42.65.Re, 42.65.Tg, 42.50.Md

I. INTRODUCTION

An optical kink is a type of soliton which can be represented as a shock wave (or shock front) with the shape preserved when propagating in a nonlinear medium [1]. In the spatial domain, such solitons are sometimes considered to be domain walls separating distinct regions of space. Kinks were mathematically introduced as solutions of the sine-Gordon equation [2] and appear in different fields of physics. In the broad sense of the word, kinks may represent not only “true” solitons with particlelike properties but also solitonic waves which can interact inelastically. In the context of optics, kinks were predicted and observed in a number of nonlinear media. Optical shock solutions were deduced for nonlinear interaction of waves via stimulated Raman scattering in both nondispersive [3] and dispersive media [4] as well as in optical fibers [5]. Kink solitons were also predicted to exist as surface waves supported by an optical lattice imprinted in a nonlinear medium [6] and in a gain medium in the presence of two-photon absorption [7]. As experimental examples, we can mention pairs of kinks and antikinks obtained in nonlinear photorefractive crystals [8], dispersive shock waves in optical fiber arrays [9], and dark solitons formed by domain walls in erbium-doped fiber lasers with birefringent cavities [10–12].

In this paper, we are interested in another type of optical-kink solution predicted by Ponomarenko and Haghgoo [13]. They have found such a solution considering the Maxwell-Bloch equations which govern the propagation of light in resonant two-level media. The kinks form as a result of self-steepening of the input waveform, which should have a constant intensity at the trailing edge. The characteristic time of the intensity jump of such an optical shock is determined by the transverse relaxation time T_2 , i.e., by relaxation of microscopic polarization. On the other hand, the longitudinal relaxation time T_1 governing the decay of the excited-state

population is responsible for kink disintegration. It turns out that these solutions possess an important property of self-similarity, i.e., scaling of their profiles during propagation. Later, the same authors confirmed the preservation of this novel type of kink under inhomogeneous broadening of the medium [14]. It is worth noting that kink solutions are absent in the media with the usual cubic (Kerr) nonlinearity and need more sophisticated situations with competing nonlinear contributions, such as cubic-quintic or saturable nonlinearity [1]. The two-level medium, being an example of a saturable absorber, supports the saturable nonlinearity which is responsible for kink formation.

This paper can be considered a continuation of the work by Ponomarenko and Haghgoo [13] and, simultaneously, a development of our previous studies of ultrashort pulses and their interactions in two-level media [15]. In particular, unusual dynamics of matter was reported under asymmetric collisions of self-induced transparency solitons [16] and in the cases of extremely short (subcycle) pulses [17] and chirped pulses [18]. However, contrary to self-induced transparency and other coherent effects which occur for ultrashort pulses, kinks form in the regime of incoherent light-matter interaction when, as stated above, the characteristic time of the input field cannot be considered negligible in comparison to relaxation times. On the other hand, consideration should differ significantly from standard steady-state analysis, which in recent decades allowed us to discover and study a number of effects such as mirrorless optical bistability [19, 20] and local-field effects [21, 22]. Although we eventually deal with stationary (constant-wave) fields, kinks are fundamentally dynamical features. Moreover, kink formation can be treated as an example of a transient process which needs full-scale modeling of temporal dynamics. Transient processes of different natures have attracted much attention in recent years, which ensures the relevance of our study for modern nonlinear optics. From the viewpoint of solitonic studies, the kinks can be considered another class of incoherent solitons along with that reported in Ref. [23].

* dnovitsky@gmail.com

Thus, in this paper, we numerically study the formation, propagation, and interaction of optical kinks in a homogeneously broadened two-level medium. The paper's structure is as follows. In Sec. II, the main equations are given, and the parameters of the calculations are discussed. Section III is devoted to the basic features of kink formation out of an input waveform; the self-similarity is tested, and kinklike pulses are introduced. In Secs. IV and V, collisions of kinks are studied with counterpropagating kinks and ultrashort pulses (solitons), respectively. The paper is completed with a short conclusion.

II. MAIN EQUATIONS AND PARAMETERS

In semiclassical approximation, light propagation in a homogeneously broadened two-level medium can be described by the Maxwell–Bloch equations. Since we deal with the incoherent regime of light-matter interaction (i.e., the characteristic time of light-intensity change is not much less than the medium relaxation times), we can safely write these equations under the rotating-wave approximation as follows (see, e.g., [15]):

$$\frac{dR}{d\tau} = i\Omega W + iR\delta - \gamma_2 R, \quad (1)$$

$$\frac{dW}{d\tau} = 2i(\Omega^* R - R^* \Omega) - \gamma_1 (W - 1), \quad (2)$$

$$\begin{aligned} \frac{\partial^2 \Omega}{\partial \xi^2} - \frac{\partial^2 \Omega}{\partial \tau^2} + 2i \frac{\partial \Omega}{\partial \xi} + 2i \frac{\partial \Omega}{\partial \tau} \\ = 3\epsilon \left(\frac{\partial^2 R}{\partial \tau^2} - 2i \frac{\partial R}{\partial \tau} - R \right), \end{aligned} \quad (3)$$

where $\tau = \omega t$ and $\xi = kz$ are the dimensionless time and distance; $\Omega = (\mu/\hbar\omega)E$ is the dimensionless electric-field amplitude (normalized Rabi frequency); E and R are the complex amplitudes of the electric field and atomic polarization, respectively; W is the difference between populations of ground and excited states; $\delta = \Delta\omega/\omega = (\omega_0 - \omega)/\omega$ is the normalized frequency detuning; ω_0 is the frequency of the atomic resonance; ω is the light's carrier frequency; μ is the dipole moment of the quantum transition; $\gamma_{1,2} = 1/(\omega T_{1,2})$ are the normalized relaxation rates of population and polarization, respectively; $\epsilon = \omega_L/\omega = 4\pi\mu^2 C/3\hbar\omega$ is the dimensionless parameter of interaction between light and matter (normalized Lorentz frequency); C is the concentration (density) of two-level atoms; $k = \omega/c$ is the wavenumber; c is the speed of light; and \hbar is the Planck constant. An asterisk stands for complex conjugation.

We solve Eqs. (1)–(3) numerically using essentially the same approach as in our previous publications (see [24]). The parameters of the medium and light used for calculations (if not stated otherwise) are listed below. The relaxation times $T_1 = 1$ ns and $T_2 = 0.1$ ps correspond to semiconductors doped with quantum dots (although we do not consider here the effects of the host medium, taking the background dielectric permittivity to be unity),

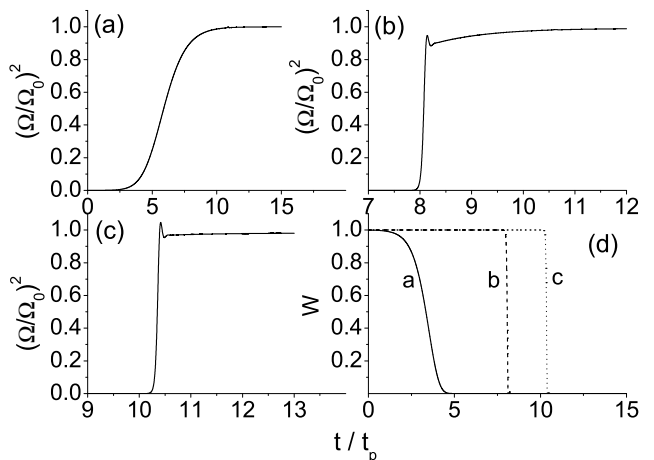


FIG. 1. Light-intensity profiles at different positions inside the medium: (a) $L = 0$, (b) $L = 500\lambda$, (c) $L = 1000\lambda$. (d) Dynamics of population difference at the same positions as in (a)–(c). The parameters of input radiation are $\Omega_0 = 0.5\gamma_2$ and $t_p = 50T_2$.

the detuning $\delta = 0$ (exact resonance, i.e., $\omega = \omega_0$), the central light wavelength $\lambda = 2\pi c/\omega_0 = 0.8 \mu\text{m}$, and the strength of light-matter coupling (the Lorentz frequency) $\omega_L = 10^{11} \text{ s}^{-1}$. The region used in calculations includes a two-level medium of thickness L surrounded by vacuum regions of length 20λ from both sides. The medium is supposed to be initially in the ground state, so that $W(t=0) = 1$.

III. KINKS AND KINK-LIKE PULSES

In this section, we consider the process of kink formation as a result of adiabatic switching of a constant wave (cw) which can be described with a functional form as follows [13]:

$$\Omega(t) = \frac{\Omega_0}{1 + e^{-(t-t_0)/t_p}}, \quad (4)$$

where Ω_0 is the normalized amplitude of the cw field at the trailing edge (Rabi frequency jump), t_p is a switching time, and t_0 is the offset time corresponding to the instant when the field amplitude is half the maximum (further, we start calculations from $t = 0$ and set $t_0 = 5t_p$ in this section). It is important that this waveform has a constant amplitude at the trailing edge. To obtain a characteristic example of the kink, we take the parameters $\Omega_0 = 0.5\gamma_2$ and $t_p = 50T_2$. Figure 1 shows the results of calculations of light-intensity dynamics at different positions inside the medium: at $L = 0$ (the entrance), $L = 500\lambda$, and $L = 1000\lambda$ (the exit). It is seen that the incident intensity changes smoothly according to the function (4). As light propagates deep inside the medium, the rising edge of the wave becomes more abrupt. This self-steepening of the wave front is a characteristic feature of kink formation. Analogous

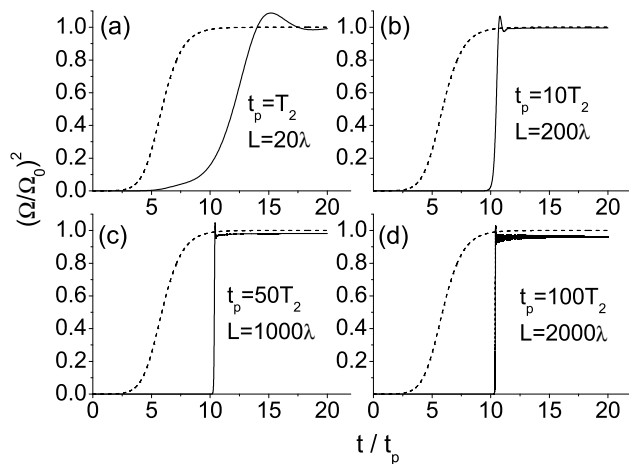


FIG. 2. Light-intensity profiles for different switching times t_p and medium thicknesses L . The Rabi frequency jump is $\Omega_0 = 0.5\gamma_2$. Dashed line shows the input waveform.

self-steepening occurs also in the dynamics of population difference at corresponding depths inside the medium [Fig. 1(d)]: the cw trailing edge rapidly saturates the medium, so that the populations of both levels become equal (hence, $W = 0$). Our kinks have another peculiarity, an overshoot (or spike) at the rising edge of the wave: for a very short time, the intensity exceeds the steady-state level at the trailing edge. This feature was absent in previous studies of kinks [13] and, perhaps, is due to chirping leading to modulations of the kink profile. We discuss this point in more detail further.

To verify that our waveforms are *the* kinks, we should demonstrate that they possess the property of self-similarity. Rather than tracing the kink profile over large distances, let us show that our waveforms can be scaled so that similar profiles can be obtained at different properly chosen parameters. According to Ref. [13], the distance of kink formation is given by

$$L_* = \frac{\Omega_\infty^2 T_2^2}{\alpha}, \quad (5)$$

where α is a linear absorption coefficient, and Ω_∞ is the asymptotic kink amplitude (Rabi frequency jump of the kink). Since $\Omega_\infty \sim \Omega_0$, $\alpha \sim T_2$, and $t_p \sim T_2$, we can expect the self-similar resulting waveforms after passing the distance

$$L \sim \Omega_0^2 T_2 \sim \Omega_0^2 t_p. \quad (6)$$

First, we fix the amplitude Ω_0 , so the input waves with t_{p1} and t_{p2} should give the same kink profile after propagating the distances related by $L_1/L_2 = t_{p1}/t_{p2}$. Figure 2 verifies this expectation at $\Omega_0 = 0.5\gamma_2$: the kinks with $t_p = 10T_2$, $50T_2$, and $100T_2$ are very similar and appear at the exit almost simultaneously (at $t = 10t_p$) after propagating $L = 200\lambda$, 1000λ and 2000λ , respectively. This observation is equivalent to self-similarity while changing the transverse relaxation rate γ_2 (or corresponding time

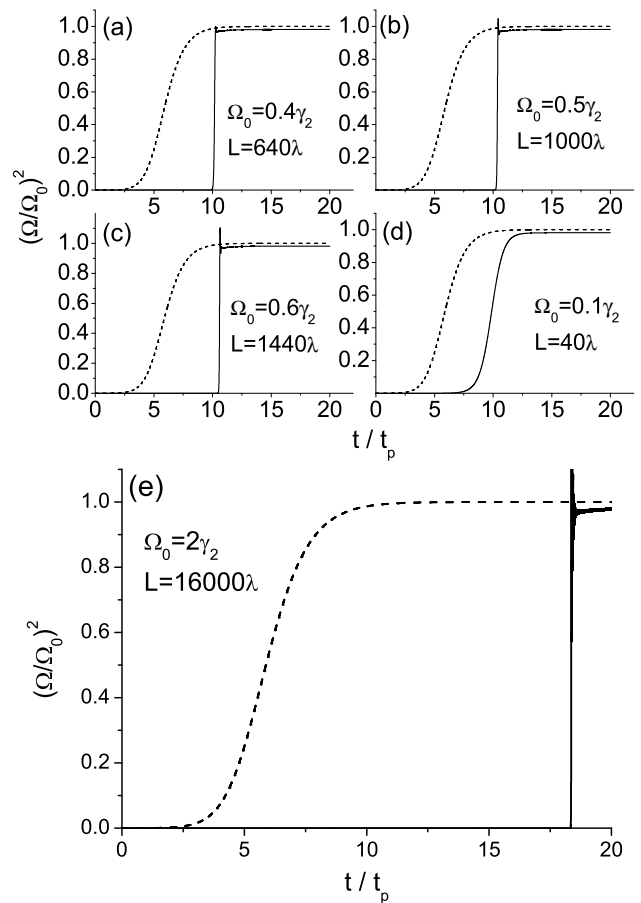


FIG. 3. Light-intensity profiles for different Rabi frequency jumps Ω_0 and medium thicknesses L . The switching time is $t_p = 50T_2$. The dashed line shows the input wave-form.

T_2). It is also seen that for a very rapid change in the input intensity, self-steepening is absent [Fig. 2(d)] since the switching time is already of the same order of magnitude as the temporal width of the kink ($t_p \sim T_2$). According to the scaling law, self-steepening could develop already after $L = 20\lambda$ but is absent even after a tenfold increase in the distance. This is direct corroboration of the expected condition $t_p \gg T_2$ for kink formation. Note also that the overshoot at the rising edge of the waveform is present in this case as well.

Second, we fix the switching time ($t_p = 50T_2$), and according to Eq. (6), the input waves with $\Omega_{0,1}$ and $\Omega_{0,2}$ should give the same kink profile after passing the distances related by $L_1/L_2 = (\Omega_{0,1}/\Omega_{0,2})^2$. The results of testing this expectation are given in Fig. 3, where the kinks with $\Omega_0 = 0.4\gamma_2$, $0.5\gamma_2$, and $0.6\gamma_2$ are shown after propagating $L = 640\lambda$, 1000λ , and 1440λ , respectively. One can see that these waveforms are very similar and need almost the same time to pass the medium (some discrepancy can be attributed to the fact that the relation $\Omega_\infty \sim \Omega_0$ is not exact). We should also note that the waveforms with higher intensity move much faster than less powerful ones. Similar kinks form at $\Omega_0 = 0.3\gamma_2$

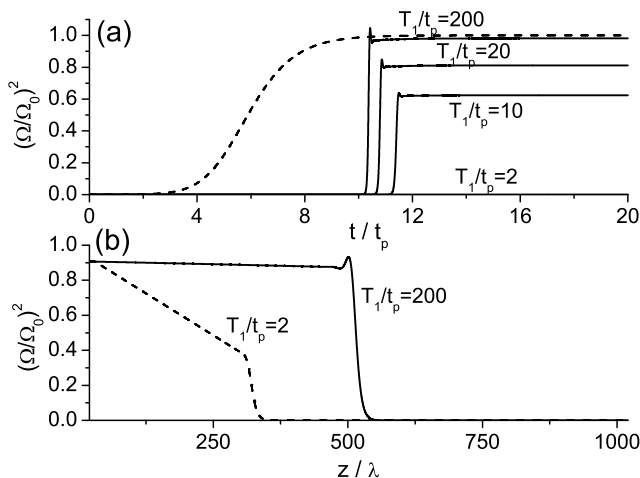


FIG. 4. (a) Light-intensity profiles and (b) intensity distributions along the medium (at time point $t = 10t_p$) for different longitudinal relaxation times T_1 . Other parameters are $\Omega_0 = 0.5\gamma_2$, $t_p = 50T_2$, $L = 1000\lambda$. The dashed line shows the input waveform.

($L = 360\lambda$) and $\Omega_0 = 0.2\gamma_2$ ($L = 160\lambda$), but as shown in Fig. 3(d), the input waveform with $\Omega_0 = 0.1\gamma_2$ cannot produce a kink after the distance $L = 40\lambda$ (or at longer distances). This is in accordance with the prediction of the critical amplitude, which gives the lower bound for kink existence [13].

On the other hand, the upper bound is given by the expression $\Omega_0 \leq 0.5\gamma_2$ [13]. At larger amplitudes, according to Ref. [13], the kink should become a chirped wave due to the onset of Rabi oscillations at larger Rabi frequencies. However, we do not see any fundamental changes in its profile at $\Omega_0 = 0.6\gamma_2$ [Fig. 3(c)]. Perhaps, the chirp appears as the spike at the rising edge of the kink which already exists at $\Omega_0 = 0.5\gamma_2$ and gradually diminishes with decreasing Ω_0 . According to our calculations, this spike appears long before the bound value of Ref. [13]: for example, it is clearly seen at $\Omega_0 = 0.4\gamma_2$ as well [Fig. 3(a)]. Thus, our numerical results show that the Rabi-oscillation-induced chirp does not become apparent abruptly at $\Omega_0 = 0.5\gamma_2$, but gradually becomes more pronounced.

What seems to be more important is that the kinks at larger Ω_0 lose the property of self-similarity despite remaining stable waveforms. This conclusion is illustrated in Fig. 3(e), which shows kink formation at $\Omega_0 = 2\gamma_2$ after propagating the distance $L = 16000\lambda$. According to Eq. (6), this waveform should be similar to those given in Figs. 3(a)-3(c), but it is not. The former need the same time ($\sim 10t_p$) to pass the medium, while the latter is much slower than expected (it needs about $17t_p$). Note that some indication of this effect was present already in Fig. 3(c), where slightly more time was required for the kink with $\Omega_0 = 0.6\gamma_2$ to propagate through the medium. Therefore, the value $\Omega_0 = 0.5\gamma_2$ can indeed be viewed as an upper bound for *self-similar* kinks.

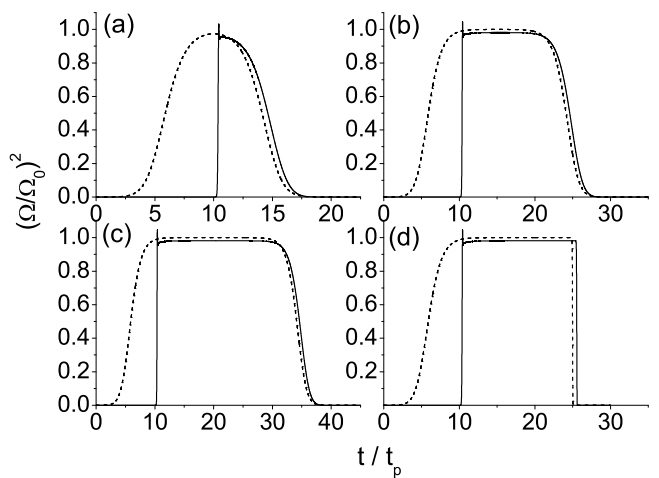


FIG. 5. Light-intensity profiles of the kink-like pulses. The parameters used are $\Omega_0 = 0.5\gamma_2$, $L = 1000\lambda$, $t_p = 50T_2$, and (a) $t'_p = 50T_2$, $t'_0 = 15t_p$; (b) $t'_p = 50T_2$, $t'_0 = 25t_p$; (c) $t'_p = 50T_2$, $t'_0 = 35t_p$; and (d) $t'_p = T_2$, $t'_0 = 25t_p$. Dashed lines show the input waveforms.

The critical lower bound of the amplitude is a function of the longitudinal relaxation time T_1 [13]. However, we will not study that dependence here. Rather, let us see how T_1 influences the kink appearance at the fixed amplitude, switching time, and medium thickness. The results of calculations at different values of T_1 are shown in Fig. 4. As the longitudinal relaxation time gets lower, the resulting Rabi frequency jump of the kink decreases as well as its speed. Finally, when $T_1 \sim t_p$, the kink entirely disappears due to energy dissipation. The decay of the field inside the medium in this case is illustrated in Fig. 4(b), in contrast to the propagating kink in the case $T_1 \gg t_p$. The dissipation of the kink can be equivalently obtained when we leave the relaxation times unchanged and consider very slowly switching waves with t_p of the same order of magnitude as T_1 .

Although it was stated that the constant intensity at the trailing edge of the input wave is a necessary condition for kink formation, this requirement is not absolute for self-steepening development. In fact, the input wave can be switched off after some time. It turns out that this time can be rather short. We model switching on and off the input light with the waveform as follows:

$$\Omega(t) = \frac{\Omega_0}{(1 + e^{-(t-t_0)/t_p})(1 + e^{(t-t'_0)/t'_p})}, \quad (7)$$

where t'_p and t'_0 are the switching-off time and the corresponding offset time, respectively, which generally differ from the switching-on characteristics t_p and t_0 . Figures 5(a)-5(c) show that the shock is formed at the rising edge of the waveform (7) even for rather short switching-off offset $t'_0 = 15t_p$ (recall that the switching-on value is $t_0 = 5t_p$) and remains essentially the same at $t'_0 = 25t_p$ and $t'_0 = 35t_p$. One can see that decay of the transmitted radiation perfectly replicates the switching-off dynamics

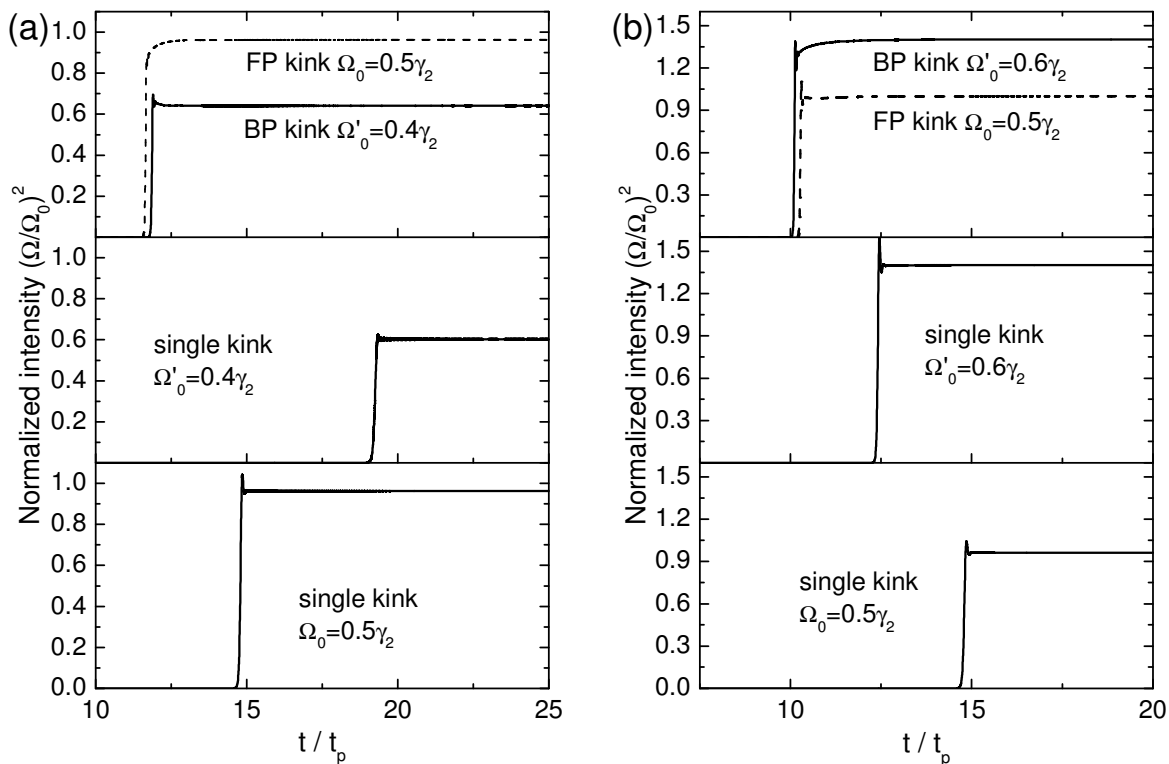


FIG. 6. Intensity profiles in the case of an interaction between the forward-propagating (FP) kink of amplitude $\Omega_0 = 0.5\gamma_2$ and the backward-propagating (BP) kink of amplitude (a) $\Omega'_0 = 0.4\gamma_2$ and (b) $\Omega'_0 = 0.6\gamma_2$ in comparison with the single-kink results. Other parameters are medium thickness $L = 2000\lambda$ and switching time $t_p = t'_p = 50T_2$ for both kinks.

of the input waveform, even for very fast switching off [$t'_p = T_2$, Fig. 5(d)]. We call such profiles formed as a result of transmission of the waveforms (7) *the kinklike pulses*.

IV. KINK-KINK INTERACTIONS

In this section, we discuss interactions between kinks or kinklike pulses. One can imagine two situations: copropagating and counterpropagating kinks. In the case of copropagating waveforms launched one after another in the same direction, the perspectives are very limited. The first waveform transforms into a kink and saturates the medium, so that the levels are equally populated, and hence, $W = 0$. Then, the second waveform propagates unchanged: since the medium is saturated, self-steepening does not occur, and the kink does not form. If the first waveform is a kinklike pulse (7), after its passing, the medium slowly returns to the ground state (with the characteristic time T_1). This means that the second waveform can be transformed into a kink if it is launched in a period long enough after the first kinklike pulse.

Let us consider a more interesting situation in which the waveforms propagate through the two-level medium in opposite directions and meet inside it. Examples of such a collision are given in Fig. 6, where one of the input

fields has the Rabi frequency jump $\Omega_0 = 0.5\gamma_2$, while the counterpropagating field is either less ($\Omega'_0 = 0.4\gamma_2$) or more ($\Omega'_0 = 0.6\gamma_2$) powerful than the first one. We choose the thickness to be large enough ($L = 2000\lambda$) that the kinks have enough time to form before collision. We compare the case of collision (top panels) with the case of single-kink formation and propagation through the medium (middle and bottom panels). One can see that the collision practically does not change the intensity of both kinks. However, the propagation speed of the kinks dramatically increases. Moreover, both kinks now move almost at the same speed. For example, the single wave-forms with $\Omega_0 = 0.5\gamma_2$ and $\Omega'_0 = 0.4\gamma_2$ need times of approximately $15t_p$ and $19t_p$ to pass the medium, while they need only about $12t_p$ in the case of the collision. Thus, we have two important facts: (i) an increase in speed propagation, and (ii) equalization of the speeds of both kinks.

This observation is due to several reasons. First, the speed of the kink depends on the stationary field intensity (Rabi frequency jump). After the collision, the kink propagates through the spatial region where the background stationary field is created by the counterpropagating waveform. In other words, the resulting intensity of the field after collision is the same and is given by the sum of amplitudes of the kinks. The raised sum intensity results in an increase in the propagation speed

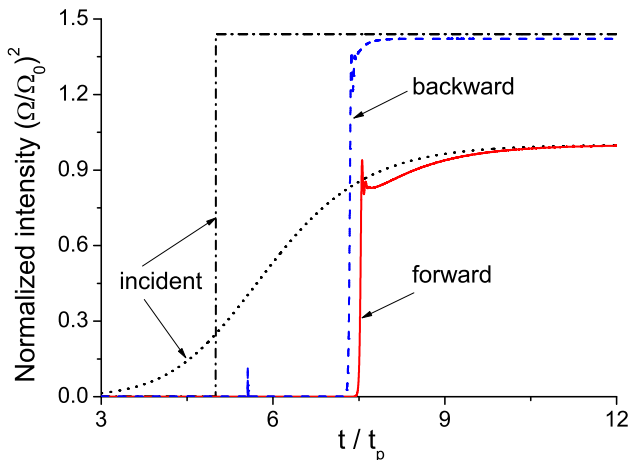


FIG. 7. (Color online) Intensity profiles in the case of an interaction between the forward-propagating (FP) kink of amplitude $\Omega_0 = 0.5\gamma_2$ and the backward-propagating (BP) wave front of amplitude $\Omega'_0 = 0.6\gamma_2$. Other parameters are medium thickness $L = 1000\lambda$ and switching time $t_p = 50T_2$ for the FP waveform and $t'_p = 0.001T_2$ for the BP waveform.

of both kinks. Second, the interaction of counterpropagating waves leads to their interference and hence to the creation of periodic grating of the population difference inside the medium [25] and even to effects of wave instability [27]. The equal speeds of both kinks can be attributed to strong interaction via this population grating, which effectively equalizes the speed of the waveforms.

Similar observations are valid for other situations, e.g., for two counterpropagating wave fronts of abruptly (not adiabatically) switched cw fields. In a sense, the increased speed of wave fronts moving apart after a collision can be interpreted as a repulsion of wave fronts or kinks. This transient process deserves a separate detailed study. Here, suffice it to say that we obtained the instrument to control the speed of the kinks which has the most impressive manifestations of kinks of comparatively low intensity: the increase in their speed after collision with more powerful kinks is the most striking.

Moreover, it is not necessary to use the kink as a backward-propagating waveform to control the forward-propagating kink. Other variants are possible as well. In Fig. 7, the results for the collision of the kink with the counterpropagating wave front switching almost instantaneously ($t'_p = 0.001T_2$) are depicted. It is seen that both waveforms pass a medium of thickness $L = 1000\lambda$ almost simultaneously and need only about $7.5t_p$ [compare with the more than $10t_p$ needed for a single kink to propagate through a medium of the same length; see Fig. 3(b)]. Another possibility is to use not the kinks, but kinklike pulses. The situation shown in Fig. 8 perfectly corresponds to the case in Fig. 6(b) where the kinks were considered. There is no need to say that we could analyze other analogous combinations, such as “a kink + a kinklike pulse” or “a kinklike pulse + a cw front”. All these situations have common features: interference of

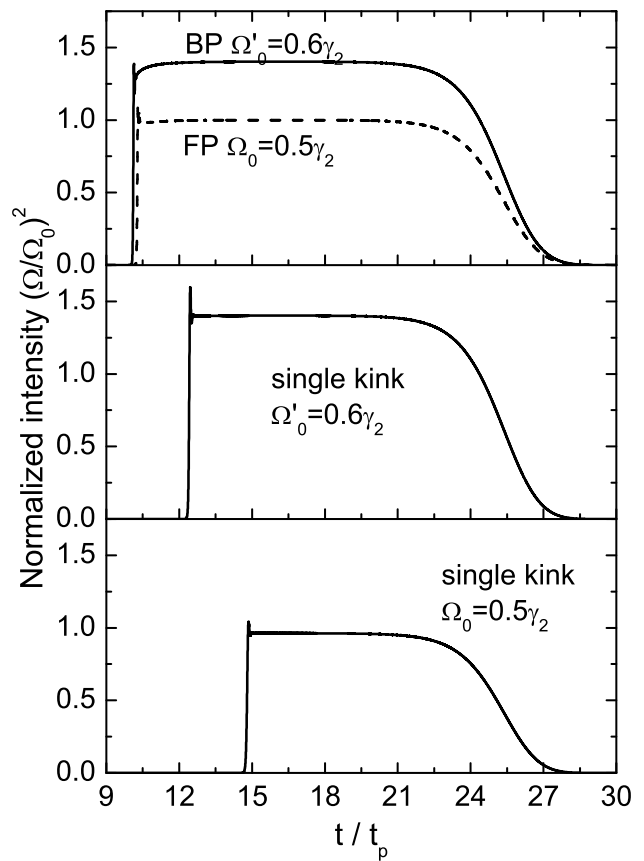


FIG. 8. Intensity profiles in the case of an interaction between the forward-propagating (FP) kinklike pulse of amplitude $\Omega_0 = 0.5\gamma_2$ and the backward-propagating (BP) kinklike pulse of amplitude $\Omega'_0 = 0.6\gamma_2$. Other parameters are medium thickness $L = 2000\lambda$ and switching time $t_p = t'_p = 50T_2$ for both kinklike pulses.

counterpropagating waves and formation of population grating.

Thus, kink propagation can be controlled with the counterpropagating waveform. What instruments do we possess to change the speed of the kink? The first such instrument is the intensity of the control (counterpropagating) waveform. This is illustrated in Fig. 6: the kink with the Rabi frequency jump $\Omega_0 = 0.5\gamma_2$ passes the medium faster after interaction with a more powerful kink ($\Omega'_0 = 0.6\gamma_2$) than with a less powerful one ($\Omega'_0 = 0.4\gamma_2$). Another instrument is the offset time t'_0 of the counterpropagating waveform. As an example, Fig. 9 shows that increasing this offset time from $5t_p$ (the backward-propagating kink is launched simultaneously with the forward-propagating one) to $8t_p$ (the backward-propagating kink is launched later than the forward-propagating one by $3t_p$) results in growing the passage time of the forward-propagating kink from about $8t_p$ to almost $9.5t_p$. The reason is obvious: the waveforms collide later, so the kink mostly propagates alone, and its passage time tends to that of a single kink (slightly over $10t_p$).

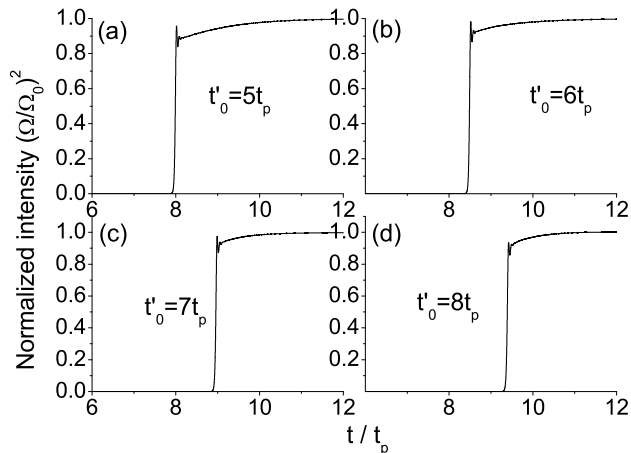


FIG. 9. Intensity profiles of the forward-propagating kink (amplitude $\Omega_0 = 0.5\gamma_2$, offset time $t_0 = 5t_p$) after an interaction with the backward-propagating kink of amplitude $\Omega'_0 = 0.6\gamma_2$ and different offset times t'_0 . Other parameters are medium thickness $L = 1000\lambda$ and switching time $t_p = t'_p = 50T_2$ for both kinks.

V. KINK-PULSE INTERACTION

In this section, we study the interaction of kinks with counterpropagating ultrashort pulses. In particular, we consider pulses of Gaussian profile $\Omega = \Omega_p \exp[-(t - t'_0)^2/2t_p'^2]$ with a duration t'_p and an offset time t'_0 . It is well known that, in the regime of coherent light-matter interaction (when $t'_p \ll T_2 \ll T_1$), such pulses form self-induced transparency (SIT) solitons [26]. The pulses considered here approximately correspond to such solitons (although the duration is only one or two orders of magnitude less than the relaxation time T_2). The key parameter of SIT solitons is their area, which at the constant t'_p , can be treated as a measure of pulse amplitude Ω_p . If the area A is equal to 2π , such a pulse inverts the medium at the rising edge and then returns it back exactly to the ground state at the trailing edge. The pulse with area differing from 2π leaves the medium partially excited and, according to the “area theorem”, can be transformed into a 2π -soliton as it propagates deep inside the medium.

Let us consider the interaction of the waveform (4) with counterpropagating pulses of different area with the duration $t'_p = 0.1T_2$ and the same offset time $t'_0 = t_p$. As in the previous section, we focus on kink speed as a parameter influenced by collision. Figure 10 shows the dependence of kink passage time on the pulse area. It is seen that there is a strong minimum around pulse area $A/2\pi = 0.84$ when the kink needs approximately $8.8t_p$ to pass a medium of $L = 1000\lambda$. At the maximum, around $A/2\pi = 1.18$, the passage time grows to $9.8t_p$, which with the parameters used, is almost equal to the value in the case of a single kink. Thus, pulse area (hence, intensity) can be considered an instrument to control the

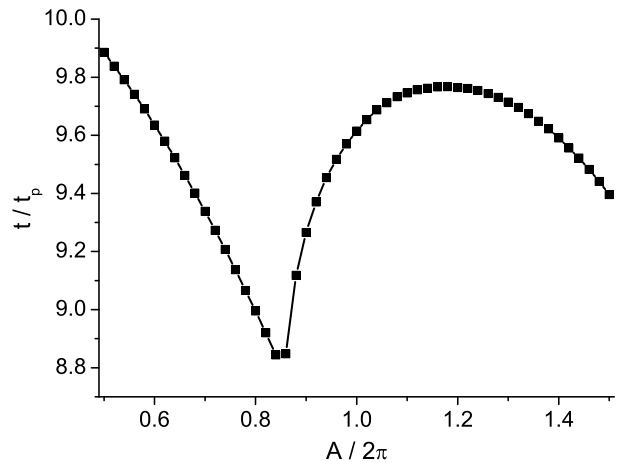


FIG. 10. Time interval needed for the forward-propagating kink to pass the medium as a function of the area of the backward-propagating pulse. Medium thickness $L = 1000\lambda$, kink switching time $t_p = 50T_2$, and Rabi frequency jump $\Omega_0 = 0.5\gamma_2$; pulse duration is $0.1T_2$, and offset time $t'_0 = t_p$.

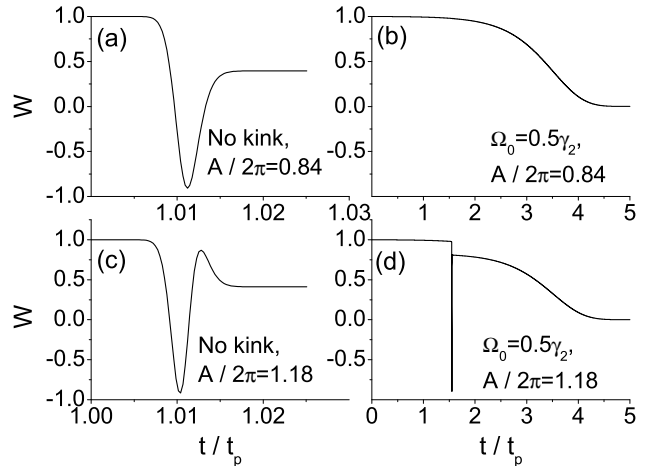


FIG. 11. Dynamics of population difference for (a) and (c) a single pulse and (b) and (d) kink-pulse interaction. Pulses of two areas are considered: (a) and (b) $A/2\pi = 0.84$, (c) and (d) $A/2\pi = 1.18$. The other parameters are the same as in Fig. 10.

kink speed.

To get insight into the interaction process, we plot in Fig. 11 the population difference at the entrance of the medium for a single pulse (no kink, left panels) and in the presence of a kink (right panels). The cases of the minimum and maximum of the curve in Fig. 10 are considered. It is seen that single pulses give approximately the same final level of population difference (around 0.4), although the one with area $A/2\pi = 1.18$ makes a complete cycle of excitation and deexcitation [Fig. 11(c)], in contrast to the one with area $A/2\pi = 0.84$ [Fig. 11(a)]. This difference between the pulses turns out to be the key factor governing their different interactions with the kink. There is a sharp dip induced by the pulse with area

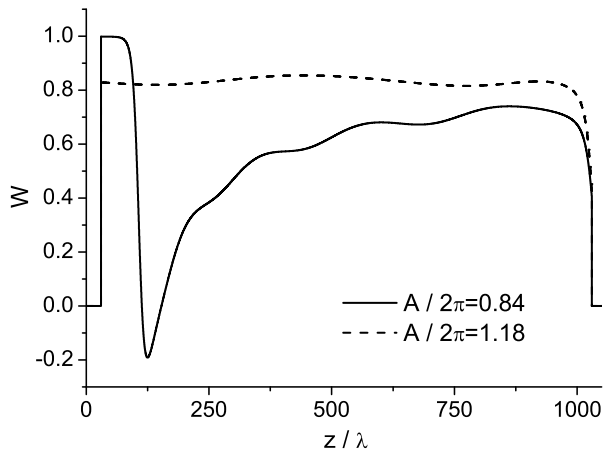


FIG. 12. Distribution of population difference along the medium for a single pulse at the time instant $t = 4t_p$. Pulses of two areas are considered: $A/2\pi = 0.84$ and 1.18 . The other parameters are the same as in Fig. 10. Note also the vacuum regions of length 20λ from both sides of the two-level medium.

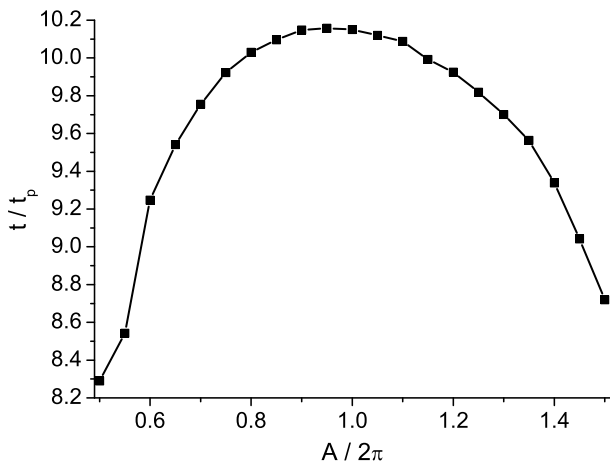


FIG. 13. Time interval needed for the forward-propagating kink to pass the medium as a function of the area of the backward-propagating pulse. Medium thickness $L = 1000\lambda$, kink switching time $t_p = 50T_2$, and Rabi frequency jump $\Omega_0 = 0.5\gamma_2$; pulse duration is $0.01T_2$, and offset time $t'_0 = t_p$.

$A/2\pi = 1.18$ and superposed on the gradual saturation of the population difference due to the kink [Fig. 11(d)]. On the contrary, the pulse with area $A/2\pi = 0.84$ does not have any visible influence on the saturation of the medium caused by the kink [Fig. 11(b)].

The reason is that the pulse with lower area has another fate even before reaching the entrance of the medium. This suggestion is confirmed by an analysis of medium excitation created by single pulses and experienced by kinks. In Fig. 12, the population difference along the medium is shown at the time instant $t = 4t_p$ when the backward-propagating pulses should already be out of the medium. The drastic difference in behavior of pulses with areas $A/2\pi = 1.18$ and 0.84 is clearly seen.

The first leaves the medium almost uniformly excited at the level of $W \sim 0.8$. The second one is strongly absorbed near the medium entrance, resulting in a profound dip while the medium near the exit (where the pulse was launched) is excited almost to the same low level as in the case of $A/2\pi = 1.18$. This is due to the fact that the condition $t'_p = 0.1T_2$ does not provide a coherent regime of light-matter interaction and formation of SIT solitons. A waveform giving rise to a kink needs more time for self-steepening and medium saturation when propagating through the strongly and nonuniformly excited medium (the case of $A/2\pi = 0.84$) than in the case of a weakly and uniformly excited one ($A/2\pi = 1.18$).

For pulses of shorter duration ($t'_p = 0.01T_2$) which better correspond to the condition of a coherent regime, we have a more obvious and predictable picture (Fig. 13). The 2π pulses which leave the medium almost unperturbed and easily transform into SIT solitons have minimal influence on the kink speed, whereas propagation of the pulses with area of π or 3π results in the maximum level of medium excitation and gives the strongest kink retardation (down to $8.3t_p$). Thus, using ultrashort counterpropagating pulses is another tool for controlling kink passage through the medium with the possibility to change the resulting kink speed with the proper choice of pulse duration and area.

VI. CONCLUSION

Using numerical simulations, we have studied in detail the formation of optical kinks and kinklike pulses in two-level media and demonstrated their self-similarity. The results are generally in agreement with the analytical theory of Ponomarenko and Haghgoo [13], although there are some minor discrepancies. In particular, the chirped kink appears in our calculations in the range of parameters where analytical theory predicts a monotonic waveform. This difference can be ascribed to our more general approach since we do not use the slowly-varying-envelope approximation. Further, we have studied collisions of kinks with other waveforms and shown that the speed of kink propagation can be significantly changed by interaction with a counterpropagating kink, stationary wave front, or ultrashort pulse. These possibilities are interesting from the physical point of view but can also be used in different optical schemes for nonlinear control of propagating wave fields and optical information processing. In particular, kinks can be considered as a substitute for the usual (pulse) solitons as optical bits of information since they can exist in different parameter ranges. We should also note that the inelasticity of collisions resulting in a speed change does not allow us to consider such kinks as strict solitons, only as solitonic waves.

In conclusion, we make several remarks on possible directions of kink studies. Although it was reported that kinks are preserved under inhomogeneous broad-

ening [14], it may be interesting to test this prediction with our more general numerical approach adapting the scheme described in Ref. [28]. Since calculations in this paper were performed for two-level atoms in vacuum, a more general consideration is worth exploring, taking into account the background matrix (see, e.g., the study of its influence on mirrorless optical bistability [29]). In a dense enough medium, near-dipole-dipole interactions between active particles begin to play an essential role, which can be taken into account through the so-called local-field correction [30]. All this allows us to consider

optical kinks an interesting example of incoherent phenomena lying between and connecting the regime of ultrafast processes (with self-induced transparency solitons being a characteristic feature) and the stationary regime (with optical bistability and similar effects). Of course, it is not less important to obtain these kinks experimentally since there are only a few practical realizations of optical shock waves and studies of their rich dynamics. The solid-state systems are especially attractive for experimental observations, in particular solids doped with resonant atoms (e.g., rare-earth ions) and bulk semiconductors doped with quantum dots.

-
- [1] Yu. S. Kivshar and G. P. Agrawal, *Optical Solitons: From Fibers to Photonic Crystals* (Academic, San Diego 2003).
- [2] L. Debnath, *Nonlinear Partial Differential Equations for Scientists and Engineers*, 2nd ed. (Birkhäuser, Boston, 2005).
- [3] D. N. Christodoulides, *Opt. Commun.* **86**, 431 (1991).
- [4] G. P. Agrawal and C. Headley III, *Phys. Rev. A* **46**, 1573 (1992).
- [5] Yu. S. Kivshar and B. A. Malomed, *Opt. Lett.* **18**, 485 (1993).
- [6] Ya. V. Kartashov, V. A. Vysloukh, and L. Torner, *Opt. Express* **14**, 12365 (2006).
- [7] A. Goyal, V. K. Sharma, T. S. Raju, and C. N. Kumar, *J. Mod. Opt.* **61**, 315 (2014).
- [8] B. Freedman, T. Carmon, M.I. Carvalho, M. Segev, and D. N. Christodoulides, *Phys. Rev. Lett.* **91**, 133902 (2003).
- [9] J. Fatome, C. Finot, G. Millot, A. Armaroli, and S. Trillo, *Phys. Rev. X* **4**, 021022 (2014).
- [10] H. Zhang, D. Y. Tang, L. M. Zhao, and X. Wu, *Phys. Rev. B* **80**, 052302 (2009).
- [11] H. Zhang, D. Y. Tang, L. M. Zhao, and X. Wu, *Phys. Rev. A* **80**, 045803 (2009).
- [12] H. Zhang, D. Y. Tang, L. M. Zhao, and X. Wu, *Opt. Express* **19**, 3525 (2011).
- [13] S. A. Ponomarenko and S. Haghgoo, *Phys. Rev. A* **82**, 051801 (2010).
- [14] S. Haghgoo and S. A. Ponomarenko, *Opt. Commun.* **286**, 344 (2013).
- [15] D. V. Novitsky, *Phys. Rev. A* **84**, 013817 (2011).
- [16] D. V. Novitsky, *Phys. Rev. A* **85**, 043813 (2012).
- [17] D. V. Novitsky, *Phys. Rev. A* **86**, 063835 (2012).
- [18] D. V. Novitsky, *Opt. Commun.* **358**, 202 (2016).
- [19] F.A. Hopf, C.M. Bowden, and W.H. Louisell, *Phys. Rev. A* **29**, 2591 (1984).
- [20] A.A. Afanas'ev, R.A. Vlasov, N.B. Gubar, and V.M. Volkov, *J. Opt. Soc. Am. B* **15**, 1160 (1998).
- [21] C.M. Bowden and J.P. Dowling, *Phys. Rev. A* **47**, 1247 (1993).
- [22] A.A. Afanas'ev, A.G. Cherstvy, R.A. Vlasov, and V.M. Volkov, *Phys. Rev. A* **60**, 1523 (1999).
- [23] A.A. Afanas'ev, R.A. Vlasov, O.K. Khasanov, T.V. Smirnova, and O.M. Fedorova, *J. Opt. Soc. Am. B* **19**, 911 (2002).
- [24] D. V. Novitsky, *Phys. Rev. A* **79**, 023828 (2009).
- [25] L. M. Narducci and N. B. Abraham, *Laser Physics and Laser Instabilities* (World Scientific, Singapore, 1988).
- [26] S.L. McCall and E.L. Hahn, *Phys. Rev.* **183**, 457 (1969).
- [27] I. Bar-Joseph and Y. Silberberg, *Phys. Rev. A* **36**, 1731 (1987).
- [28] D. V. Novitsky, *J. Phys. B* **47**, 095401 (2014).
- [29] D. V. Novitsky, *J. Opt. Soc. Am. B* **28**, 18 (2011).
- [30] D. V. Novitsky, *Phys. Rev. A* **82**, 015802 (2010).